

Technical Notes

TECHNICAL NOTES are short manuscripts describing new developments or important results of a preliminary nature. These Notes should not exceed 2500 words (where a figure or table counts as 200 words). Following informal review by the Editors, they may be published within a few months of the date of receipt. Style requirements are the same as for regular contributions (see inside back cover).

Analysis of 3-D Conduction–Radiation Heat Transfer Using the Lattice Boltzmann Method

Bittagopal Mondal* and Subhash C. Mishra†
Indian Institute of Technology Guwahati,
Guwahati 781 039, India

DOI: 10.2514/1.37948

Nomenclature

b	=	number of discrete directions
C	=	clustering parameter
c_p	=	specific heat, kJ/kgK
\mathbf{e}_i	=	velocity, m/s
G	=	incident radiation, W/m ²
k	=	thermal conductivity, W/mK
L	=	reference length, m
N	=	conduction–radiation parameter
n	=	n th lattice center/control volume
n_i	=	particle distribution function, K
$n_i^{(eq)}$	=	equilibrium particle distribution function, K
Q^m	=	volumetric heat generation rate, W/m ³
q_C	=	conductive heat flux, W/m ²
q_R	=	radiative heat flux, W/m ²
\mathbf{r}	=	position, $r(x, y, z)$, m
T	=	temperature, K
t	=	time, s
U	=	speed, m/s
w_i	=	weight for i th direction
X, Y, Z	=	length of the medium in x, y , and z directions, m
x_n, y_n, z_n	=	coordinates of the n th lattice center or control volume, m
α	=	thermal diffusivity, m ² /s
β	=	extinction coefficient, m ^{−1}
ε	=	emissivity
ζ	=	nondimensional time, $\alpha\beta^2 t$
θ	=	nondimensional temperature
ρ	=	density, kg/m ³
τ	=	relaxation time, s
Ψ	=	nondimensional heat flux
ω	=	scattering albedo

Subscripts

B	=	back
C	=	conductive
E	=	east
F	=	front
i	=	direction
N	=	north
n	=	n th lattice/control volume
o	=	at initial time
R	=	radiative
ref	=	reference
S	=	south
T	=	total
W	=	west
x, y, z	=	x, y , and z directions

Superscripts

(eq)	=	equilibrium
*	=	nondimensional

I. Introduction

IN THE recent past, the lattice Boltzmann method (LBM) has found extensive applications in fluid mechanics [1], and its application to heat transfer problems has been encouraging [1–5]. Mishra and Lankadasu [3], Mishra and Roy [4], and Mondal and Mishra [5] have recently extended the applications of the LBM in solving heat transfer problems involving thermal radiation. They have analyzed various types of problems in 1-D planar and 2-D rectangular geometries [3–5].

Recently Talukdar et al. [6] used the finite volume method (FVM) to solve a conduction–radiation problem in a 3-D cubical enclosure. Wellele et al. [7] have analyzed several problems with nonuniform heating for the conduction–radiation problem in a 3-D rectangular enclosure. However, as far as analysis of conduction–radiation problems in 3-D geometries using the LBM is concerned, no study has been reported so far. The present work is, therefore, aimed at extending the application of the LBM to solve transient conduction–radiation problems in a 3-D cubical enclosure containing a participating medium in which the FVM is used to compute the radiative information. To generalize the usage of the LBM, a test problem is solved on both uniform and nonuniform lattices/control volumes. Further, cases of constant temperature as well as heat flux boundary conditions are also considered. The effect of heat generation is taken into account. To check the performance of the LBM–FVM on nonuniform lattices/control volumes, comparisons of temperature results have been made for various parameters.

II. Formulation

A 3-D cubical absorbing, emitting, and scattering homogeneous medium is initially at temperature T_E . For time $t > 0$, its south boundary is subjected to a constant temperature T_S or a constant heat flux $q_{T,S}$. Other boundaries remain at the initial temperature T_E . The medium can have a volumetric heat generation source. With thermophysical and optical properties constant, for the problem under consideration, in the LBM, the equation describing conduction–radiation heat transfer with volumetric heat generation

Received 8 April 2008; revision received 29 September 2008; accepted for publication 29 September 2008. Copyright © 2008 by Bittagopal Mondal and Subhash C. Mishra. Published by the American Institute of Aeronautics and Astronautics, Inc., with permission. Copies of this paper may be made for personal or internal use, on condition that the copier pay the \$10.00 per-copy fee to the Copyright Clearance Center, Inc., 222 Rosewood Drive, Danvers, MA 01923; include the code 0887-8722/09 \$10.00 in correspondence with the CCC.

*Ph.D. Student, Department of Mechanical Engineering.

†Professor, Department of Mechanical Engineering; scm_iitg@yahoo.com.

is given by [3,4]:

$$n_i(\mathbf{r} + \mathbf{e}_i \Delta t, t + \Delta t) = n_i(\mathbf{r}, t) - \frac{\Delta t}{\tau} \left[n_i(\mathbf{r}, t) - n_i^{(\text{eq})}(\mathbf{r}, t) \right] - \left(\frac{\Delta t w_i}{\rho c_p} \right) \nabla \cdot \mathbf{q}_R + \Delta t w_i \dot{Q}''', \quad i = 0, 1, 2, \dots, b \quad (1)$$

In Eq. (1), $\nabla \cdot \mathbf{q}_R$ that accounts for the volumetric radiation is given by

$$\nabla \cdot \mathbf{q}_R = (1 - \omega) \beta \left[4\pi \left(\frac{\sigma T^4}{\pi} \right) - G \right] \quad (2)$$

In the present work, the radiative term $\nabla \cdot \mathbf{q}_R$ is computed using the FVM and its methodology can be found in Mishra and Roy [4].

The relaxation time τ appearing in Eq. (1) for the D3Q15 lattice is given by

$$\tau = \frac{3\alpha}{|\mathbf{e}_i|^2} + \frac{\Delta t}{2} \quad (3)$$

where the 15 velocities \mathbf{e}_i for the D3Q15 lattice are given by

$$\begin{aligned} e_0 &= (0, 0, 0), & e_{1,2} &= (\pm 1, 0, 0) \cdot U, & e_{3,4} &= (0, \pm 1, 0) \cdot U \\ e_{5,6} &= (0, 0, \pm 1) \cdot U, & e_{7,8,\dots,14} &= (\pm 1, \pm 1, \pm 1) \cdot U \end{aligned} \quad (4)$$

where for a square lattice $U = \frac{\Delta x}{\Delta t} = \frac{\Delta y}{\Delta t} = \frac{\Delta z}{\Delta t}$. In the present problem, temperature is computed from

$$T(\mathbf{r}, t) = \sum_{i=0}^b n_i(\mathbf{r}, t) \quad (5)$$

To process Eq. (1), the required equilibrium distribution function $n_i^{(\text{eq})}$ is given by

$$n_i^{(\text{eq})}(\mathbf{r}, t) = w_i T(\mathbf{r}, t) \quad (6)$$

For the 15 velocities given in Eq. (4), the corresponding weights are

$$w_i = \begin{cases} \frac{2}{9} & \text{if } i = 0 \\ \frac{1}{9} & \text{if } 1 \leq i \leq 6 \\ \frac{1}{72} & \text{if } 7 \leq i \leq 14 \end{cases} \quad (7)$$

With nondimensional distance r^* , temperature θ , conduction-radiation parameter N , incident radiation G^* , time ζ , radiative heat flux $\Psi_R = \frac{q_R}{\sigma T_{\text{ref}}^4}$, and heat generation rate \dot{Q}'''^* defined in the following way:

$$\begin{aligned} r^* &= \frac{r}{L_{\text{ref}}} & \theta &= \frac{T}{T_{\text{ref}}} & N &= \frac{k\beta}{4\sigma T_{\text{ref}}^3} & G^* &= \frac{G}{\left(\frac{\sigma T_{\text{ref}}^4}{\pi} \right)} \\ \zeta &= \alpha \beta^2 t & \dot{Q}'''^* &= \frac{\dot{Q}'''}{k T_{\text{ref}} \beta^2} \end{aligned} \quad (8)$$

in nondimensional form, Eq. (1) is written as

$$\begin{aligned} n_i^*(\mathbf{r}^* + \mathbf{e}_i^* \Delta \zeta, \zeta + \Delta \zeta) &= n_i^*(\mathbf{r}^*, \zeta) - \frac{\Delta \zeta}{\tau^*} [n_i^*(\mathbf{r}^*, \zeta) - n_i^{*(\text{eq})}(\mathbf{r}^*, \zeta)] \\ &\quad - \left(\frac{\Delta t w_i}{4N} \right) \nabla \cdot \Psi_R + \Delta t w_i \dot{Q}'''^* \end{aligned} \quad (9)$$

where in Eq. (9) $\nabla \cdot \Psi_R$ is given by

$$\nabla \cdot \Psi_R = 4(1 - \omega) \left[\theta^4 - \frac{G^*}{4\pi} \right] \quad (10)$$

and in Eq. (9) nondimensional relaxation time τ^* is given by

$$\tau^* = \frac{3}{|\mathbf{e}_i^*|^2} + \frac{\Delta \zeta}{2} \quad (11)$$

where $\mathbf{e}_i^* = \frac{\Delta \mathbf{r}^*}{\Delta \zeta}$ is the nondimensional velocity.

For 1-D and 2-D geometries, implementations of the temperature boundary conditions in the LBM have been explained in Mishra and Lankadasu [3] and that of the flux boundary condition in Mondal and Mishra [5]. In the present work, while implementing the boundary conditions for the 3-D geometries, procedures described in [3,5] have been followed.

III. Results and Discussion

In the present work, the nonuniform size lattices/control volumes were generated from the following expressions:

$$x_n = \left\{ \frac{n-1}{N_x} + \frac{C_x}{\pi} \sin \left(\frac{\pi(n-1)}{N_x} \right) \right\} \quad (12)$$

$$y_n = \left\{ \frac{n-1}{N_y} + \frac{C_y}{\pi} \sin \left(\frac{\pi(n-1)}{N_y} \right) \right\} \quad (13)$$

$$z_n = \left\{ \frac{n-1}{N_z} + \frac{C_z}{\pi} \sin \left(\frac{\pi(n-1)}{N_z} \right) \right\} \quad (14)$$

where x_n , y_n , and z_n are the coordinates of the lattice center in the LBM and the control volume corner in the FVM in x -, y -, and z -directions, respectively. N_x , N_y , and N_z are the total number of lattices/control volumes in the x -, y -, and z -directions, respectively, and C_x ($0 \leq |C_x| \leq 1$), C_y ($0 \leq |C_y| \leq 1$), and C_z ($0 \leq |C_z| \leq 1$) are the parameters that determine clustering. With $C_x = 0$, $C_y = 0$, and $C_z = 0$, uniform size lattices/control volumes are obtained.

In the problems considered in the present work, a 3-D cubical absorbing, emitting, and isotropic scattering medium of unit length was considered. For grid and ray independency tests, numerical experiments were performed with $21 \times 21 \times 21$, $31 \times 31 \times 31$, $41 \times 41 \times 41$, and $51 \times 51 \times 51$ lattices/control volumes and 4×8 , 6×8 , 8×8 , and 10×8 ray directions over the spherical space in the FVM. No significant changes in results were observed beyond $31 \times 31 \times 31$ lattices and 8×8 ray directions. In all the cases, nondimensional time step $\Delta \xi = \alpha \beta^2 t = 1.0 \times 10^{-4}$ was used, and the steady-state condition was assumed to have been achieved when the maximum variation in temperature $\theta = \frac{T}{T_{\text{ref}}}$ at any location between two consecutive time levels did not exceed 1.0×10^{-6} . In the following, we provide results of 3 test cases:

Case 1: Transient conduction-radiation in a 3-D cubical enclosure with a constant temperature boundary condition. Initially the 3-D cubical absorbing, emitting, and isotropically scattering medium is at temperature θ_0 . For time $\zeta > 0$, its south ($\frac{y}{Y} = 0$) boundary is maintained at temperature $\theta_s = 2\theta_0$. With the south boundary temperature T_s set as the reference temperature $T_{\text{ref}} = T_s$, for the problem under consideration, $\theta_s = 1.0$ and temperatures of the rest of the boundaries are $\theta_0 = \theta_N = \theta_W = \theta_E = \theta_F = \theta_B = 0.5$. The problem is solved for the uniform and nonuniform lattices/control volumes.

In Figs. 1a–1h, at different time levels $\zeta (= \alpha \beta^2 t)$, for both uniform and nonuniform lattices, centerline ($\frac{x}{X} = 0.5, \frac{y}{Y} = 0, \frac{z}{Z} = 0.5$) temperature θ distributions along the y direction obtained from the LBM–FVM have been compared for the effects of different radiative parameters. In all of the cases, the steady-state θ results of the present work have been compared with Talukdar et al. [6].

With $\omega = 0.0$ and $N = 0.01$, and considering all boundaries black ($\varepsilon = 1.0$), θ distributions have been compared in Figs. 1a and 1b for the extinction coefficients $\beta = 0.1$ and 5.0 , respectively. The number of iterations for the steady-state solutions with nonuniform lattices for $\beta = 0.1$ and 5.0 were found 2573 and 200, respectively. The number of iterations for uniform lattices were 2553 and 203.

With $\beta = 1.0$ and $N = 0.01$, and considering all boundaries black ($\varepsilon = 1.0$), for the scattering albedo $\omega = 0.5$ and 0.9 , results have been shown in Figs. 1c and 1d, respectively. For nonuniform lattices, the number of iterations for the steady-state solution were found to be 1230 and 2078 for $\omega = 0.5$ and 0.9 , respectively. The number of iterations for uniform lattices were 1219 and 2073.

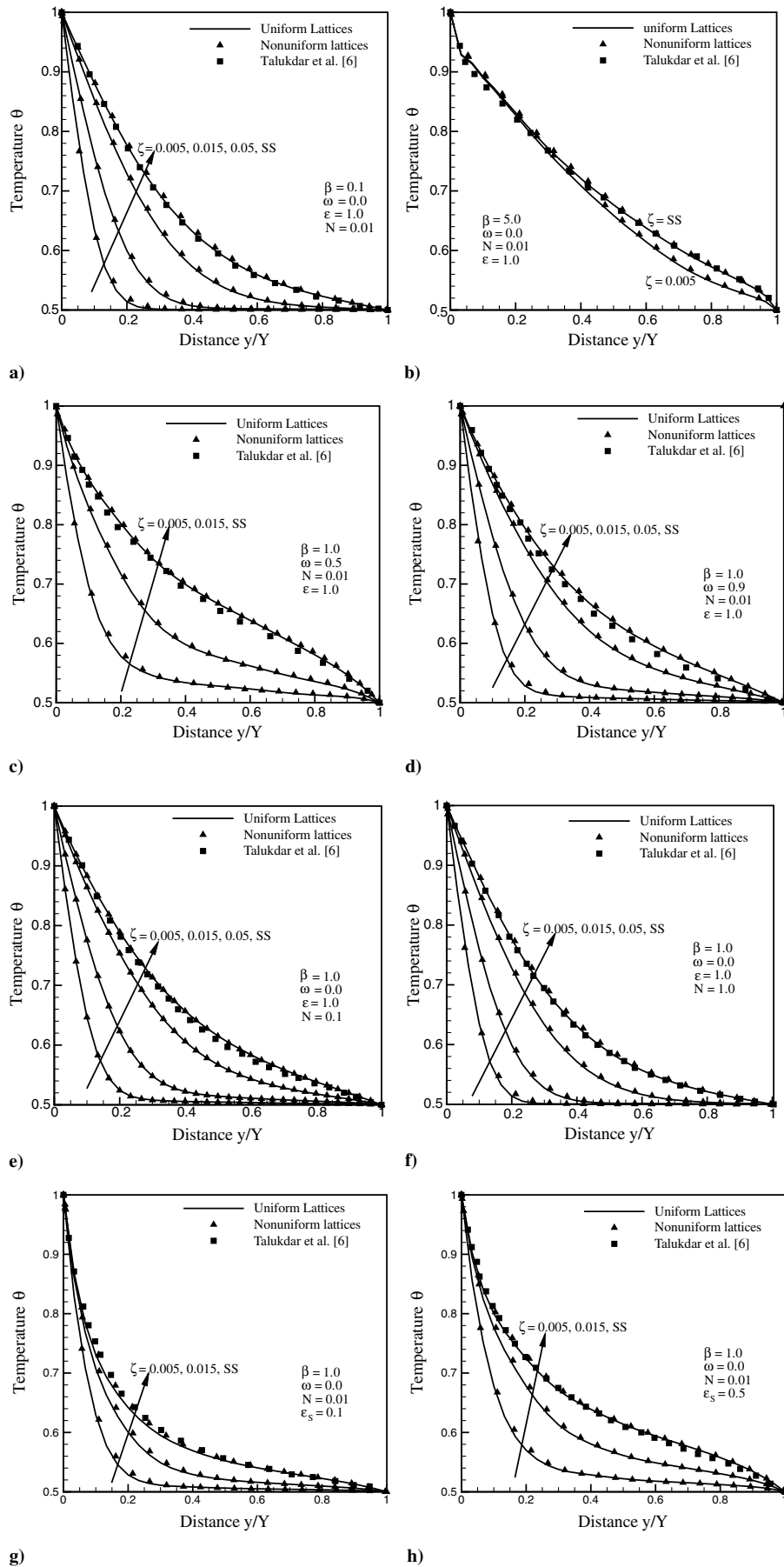


Fig. 1 Comparison of center line ($\frac{x}{X} = 0.5, \frac{y}{Y} = \frac{z}{Z} = 0.5$) temperature θ at different instants ζ for different sets of radiative parameters with all boundaries at prescribed temperatures (case 1).

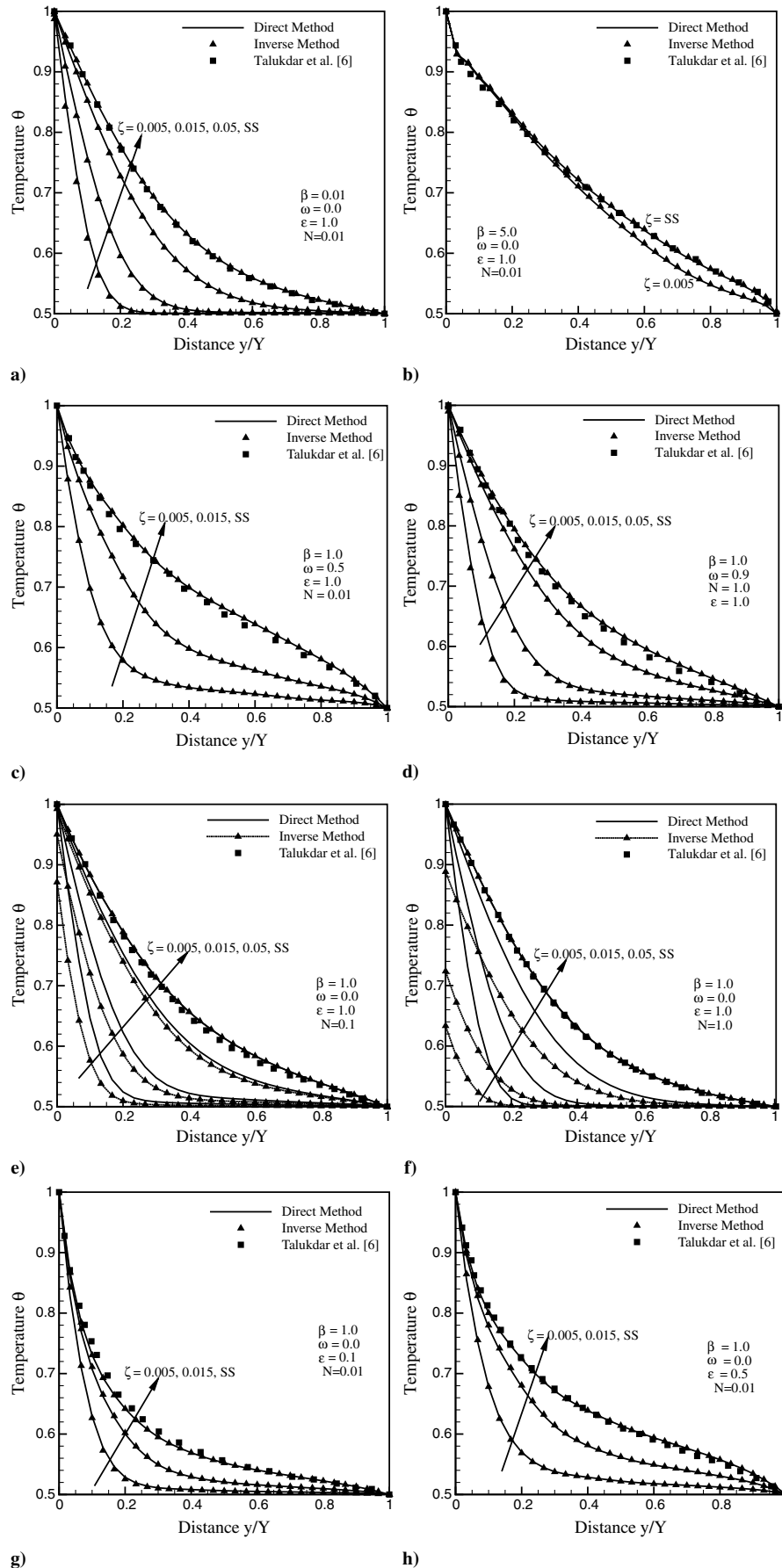


Fig. 2 Comparison of center line ($\frac{x}{X} = 0.5, \frac{y}{Y} = 0.5, \frac{z}{Z} = 0.5$) temperature θ at different instants ζ for different sets of radiative parameters with imposed heat flux at the south boundary (case 2).

In Figs. 1e and 1f, results have been shown for the conduction–radiation parameters $N = 0.1$ and 1.0 , respectively. Other radiative parameters are $\beta = 1.0$, $\omega = 0.0$, and $\varepsilon = 1.0$. In case of nonuniform lattices, for $N = 0.1$ and 1.0 , the number of iterations for steady-state solutions were found to be 2225 and 2590, respectively. The number of iterations for the uniform lattices were 2217 and 2569.

In Figs. 1g and 1h, with $\beta = 1.0$, $\omega = 0.0$, and $N = 0.01$, results are shown for south boundary emissivities of $\varepsilon_s = 0.1$ and 0.5 , respectively. Other boundaries are considered black. For nonuniform lattices, the number of iterations for the steady-state results were 993 and 941, respectively. The number of iterations for the uniform lattices were 993 and 944.

In all the cases considered in Figs. 1a–1h, at all times ζ , results of the uniform and nonuniform lattices were found to be in good agreement, and the steady-state results of the present work matched very well with the results of Talukdar et al. [6].

Case 2: Conduction–radiation in a 3-D cubical enclosure with one boundary at a prescribed heat flux: The 3-D cubical absorbing,

emitting, and isotropically scattering medium, with diffuse-gray boundaries, is initially at temperature θ_0 . For time $\zeta > 0$, its south boundary is subjected to heat flux $\Psi_{T,S}$, and the rest of the boundaries remain at temperature θ_0 .

To validate the LBM–FVM formulation and its implementation for the heat flux boundary condition for a transient conduction–radiation problem, we first solved the direct problem. In the direct problem, for a prescribed boundary temperature, the total heat flux $\Psi_{T,S} = \Psi_C + \Psi_R$ at the south boundary is calculated. Then in the inverse problem, the computed value of heat flux $\Psi_{T,S}$ became the imposed heat flux at the south boundary. All other boundaries remain at the prescribed temperature as in the case of the direct problem. With other parameters and conditions remaining the same, the validation of the LBM–FVM with the flux boundary condition is established if both the direct method and inverse method yield the same results.

In Figs. 2a–2h, the LBM–FVM formulation was validated by comparing the centerline ($\frac{x}{X} = 0.5, \frac{y}{Y}, \frac{z}{Z} = 0.5$) temperature θ

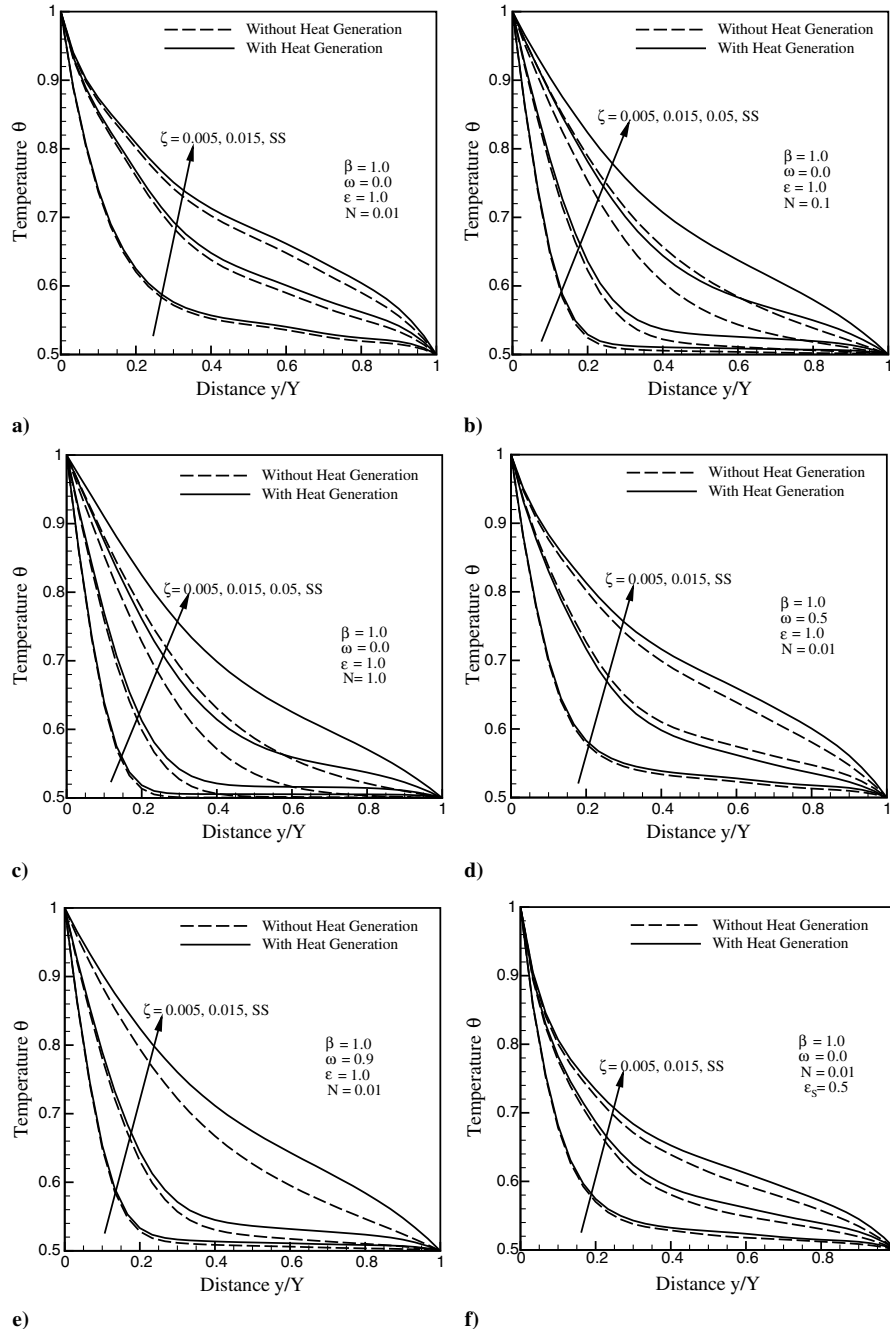


Fig. 3 Comparison of center line ($\frac{x}{X} = 0.5, \frac{y}{Y}, \frac{z}{Z} = 0.5$) temperature θ results with and without heat generation at different instants ζ for different sets of radiative parameters (case 3).

obtained from the direct method and the inverse method. Comparisons have been made at different time ζ levels including the steady state. Steady-state results were compared with Talukdar et al. [6].

With $\omega = 0.0$, $N = 0.01$, and all boundaries black $\varepsilon = 1.0$, in Figs. 2a and 2b, centerline θ results have been compared for extinction coefficients $\beta = 0.01$ and 5.0, respectively. For $\beta = 0.01$ and 5.0, in the inverse method, the number of iterations for the steady-state results were found to be 2073 and 200, respectively. The number of iterations in the direct method were 2563 and 204.

In Figs. 2c and 2d, centerline θ results have been compared for $\omega = 0.5$ and 0.9, respectively. For these results, values of other parameters are $\beta = 1.0$, $N = 0.01$, and $\varepsilon = 1.0$. In the inverse method, for $\omega = 0.5$ and 0.9, the numbers of iterations for steady-state solution were 1086 and 1759, respectively. The numbers of iterations for the direct method were 1219 and 2073.

In Figs. 2e and 2f, θ results have been shown for $N = 0.1$ and 1.0, respectively. Here values of other parameters are $\beta = 1.0$, $\omega = 0.0$, and $\varepsilon = 1.0$. In the conduction-dominated case ($N = 1.0$) (Fig. 2f), in the inverse method, temperature θ evolution is slow. This is because in the inverse method, with prescribed heat flux $\Psi_{T,S}$ at the south boundary, temperature θ at the south boundary is calculated. At this boundary, θ evolves from a low value to the correct value, which is unity. On the other hand, in the direct method, temperature θ of the south boundary is prescribed. In the radiation-dominated case ($N = 0.1$) (Fig. 2e), radiation augments temperature evolution and, thus, unlike Fig. 2f in this case, in the inverse method, θ profiles do not lag much behind those of the direct method. For $N = 0.1$ and 1.0, in the inverse method, the number of iterations for the steady-state results were 1921 and 2567, respectively. The number of iterations in the direct method were 2217 and 2569.

With $\beta = 1.0$, $\omega = 0.0$, and $N = 0.01$, in Figs. 2g and 2h, centerline θ results computed from the direct and inverse methods have been compared for the two values of the south boundary emissivity $\varepsilon_s = 0.1$ and 0.5, respectively. In the inverse method, for $\varepsilon_s = 0.1$ and 0.5, the numbers of iterations for the steady-state results were found to be 890 and 858, respectively. The number of iterations in the direct method were 993 and 944.

It is seen from Figs. 2a–2h that in all the cases, results of the direct and the inverse methods match with each other well and the steady-state results are in good agreement with Talukdar et al. [6].

Case 3: Conduction–radiation in a 3-D cubical enclosure with constant temperature boundary condition and volumetric heat generation: Initially the 3-D cubical absorbing, emitting, and isotropically scattering medium is at temperature θ_0 and for time $\zeta > 0$, its south boundary is maintained at a constant temperature $\theta_s = 2\theta_0$ and the rest of the boundaries are at temperature θ_0 . A nondimensional volumetric heat generation of unity is considered within the medium.

In Figs. 3a–3f, centerline ($\frac{x}{L} = 0.5, \frac{y}{L}, \frac{z}{L} = 0.5$) temperature θ distributions in the medium with and without heat generation have been compared. With $\beta = 1.0$, $\omega = 0.0$, and $\varepsilon = 1.0$, in Figs. 3a–3c, results have been compared for $N = 0.01$, 0.1, and 1.0, respectively. It is observed from Figs. 3a–3c that in the radiation-dominated case ($N = 0.01$) (Fig. 3a), heat generation does not have much effect on θ . In conduction-dominated case ($N = 1.0$) (Fig. 3c), the θ profile is steeper compared with the radiation-dominated case ($N = 0.01$) (Fig. 3a).

In Figs. 3d and 3e, for $\omega = 0.5$ and 0.9, with and without heat generation, θ distributions have been studied. For results in both of these figures, $\beta = 1.0$, $N = 0.01$, and $\varepsilon = 1.0$. It is observed from

these figures that the effect of heat generation on θ distribution is more pronounced when the medium has more scattering ($\omega = 0.9$). In Fig. 3f, with south boundary emissivity $\varepsilon_s = 0.5$, with and without heat generation, θ distributions have been studied. For results in this figure, $\beta = 1.0$, $N = 0.01$, and $\omega = 0.0$. A comparison of Figs. 3a and 3f shows that when the south boundary is more reflecting ($\varepsilon_s = 0.5$), the effect of heat generation gives a slightly higher temperature.

IV. Conclusions

The LBM in conjunction with the FVM was used for the solution of combined conduction–radiation problems in a 3-D cubical absorbing, emitting, and isotropically scattering medium. Both temperatures as well as flux boundary conditions were considered. Volumetric heat generation was taken into account. Centerline temperature distributions were obtained for various parameters. With all boundaries at prescribed temperatures, in all the cases, results of uniform and nonuniform lattices/control volumes were also compared and steady-state results were compared with those available in the literature. Results were found to be in good agreement. Numbers of iterations for steady-state solutions were comparable for both uniform and nonuniform lattices. With the south boundary at a prescribed heat flux, the LBM–FVM formulation was validated by comparing temperature results of both the direct and inverse methods. In this case, in the inverse method, the number of iterations for the steady-state solution was found to be less. In conduction-dominated cases, heat generation was found to have a significant effect on temperature.

References

- [1] Chen, S., and Doolen, G. D., “Lattice Boltzmann Method for Fluid Flows,” *Annual Review of Fluid Mechanics*, Vol. 30, No. 1, 1998, pp. 329–364.
doi:10.1146/annurev.fluid.30.1.329
- [2] Jiaung, W. S., Ho, J. R., and Kuo, C. P., “Lattice Boltzmann Method for Heat Conduction Problem with Phase Change,” *Numerical Heat Transfer: Part B, Fundamentals*, Vol. 39, No. 2, 2001, pp. 167–187.
doi:10.1080/10407790150503495
- [3] Mishra, S. C., and Lankadasu, A., “Analysis of Transient Conduction and Radiation Heat Transfer Using the Lattice Boltzmann Method and the Discrete Transfer Method,” *Numerical Heat Transfer, Part A*, Vol. 47, No. 9, 2005, pp. 935–954.
doi:10.1080/10407780590921935
- [4] Mishra, S. C., and Roy, H. K., “Solving Transient Conduction–Radiation Problems Using the Lattice Boltzmann Method and the Finite Volume Method,” *Journal of Computational Physics*, Vol. 223, No. 1, 2007, pp. 89–107.
doi:10.1016/j.jcp.2006.08.021
- [5] Mondal, B., and Mishra, S. C., “The Lattice Boltzmann Method and the Finite Volume Method Applied to Conduction–Radiation Problems with Heat Flux Boundary Conditions,” *International Journal of Numerical Methods in Engineering* (to be published). doi:10.1002/nme.2482
- [6] Talukdar, P., Issendorff, F. V., Trimis, D., and Simonson, C. J., “Conduction–Radiation Interaction in 3-D Irregular Enclosures Using the Finite Volume Method,” *Heat and Mass Transfer*, Vol. 44, No. 6, 2008, pp. 695–704.
doi:10.1007/s00231-007-0303-2
- [7] Wellele, O., Orlande, H. R. B., Ruperti, N., Jr., Colaco, M. J., and Delmas, A., “Coupled Conduction–Radiation in Semi-Transparent Materials at High Temperatures,” *Journal of Physics and Chemistry of Solids*, Vol. 67, Nos. 9–10, 2006, pp. 2230–2240.
doi:10.1016/j.jpcs.2006.06.007